JACS
JOURNAL OF THE AMERICAN CHEMICAL SOCIETY

Communication

pubs.acs.org/JACS

Crossing the Insulator-to-Metal Barrier with a Thiazyl Radical Conductor

Aaron Mailman,[†] Stephen M. Winter,[†] Xin Yu,[†] Craig M. Robertson,[‡] Wenjun Yong,[#] John S. Tse,[§] Richard A. Secco,[#] Zhenxian Liu,[⊥] Paul A. Dube,[∥] Judith A. K. Howard,[‡] and Richard T. Oakley*[,†]

[†]Department of Chemistry, University of Waterloo, Waterloo, Ontario N2L 3G1, Canada

[‡]Department of Chemistry, University of Durham, Durham DH1 3LE, U.K.

[#]Department of Earth Sciences, University of Western Ontario, London, Ontario N6A 5B7, Canada

[§]Department of Physics and Engineering Physics, University of Saskatchewan, Saskatoon, Saskatchewan S7N 5E2, Canada

[⊥]Geophysical Laboratory, Carnegie Institution of Washington, 5251 Broad Branch Road NW, Washington, D.C. 20015, United States

[∥]Brockhouse Institute for Materials Research, McMaster University, Hamilton, Ontario L8S 4M1, Canada

Supporting Information

ABSTRACT: The layered-sheet architecture of the crystal structure of the fluoro-substituted oxobenzene-bridged bisdithiazolyl radical FBBO affords a 2D π-electronic structure with a large calculated bandwidth. The material displays high electrical conductivity for a $f = {}^1/_2$ system, with $\sigma(300\ \mathrm{K}) = 2 \times 10^{-2}$ S cm^{-1}. While the conductivity is thermally activated at ambient pressure, with $E_{act} = 0.10$ eV at 300 K, indicative of a Mott insulating state, E_{act} is eliminated at 3 GPa, suggesting the formation of a metallic state. The onset of metallization is supported by infrared measurements, which show closure of the Mott-Hubbard gap above 3 GPa.

The possibility that the unpaired electron present in a neutral organic radical could serve as a carrier of charge was first suggested by Haddon.[1] Ideally, an array of radicals, interacting through their singly occupied molecular orbitals (SOMOs), would give rise to a half-filled ($f = {}^1/_2$) energy band, and possess a metallic ground state. The problem with the model stems from the intrinsically high Coulombic barrier U to charge transfer in this (or any other)[2] $f = {}^1/_2$ system. When this barrier dominates, the unpaired electrons are localized, and simple organic radicals like aminyls, nitroxyls, and verdazyls are Mott insulators.[3] Overcoming the onsite charge repulsion requires radicals with extensive spin delocalization to lower U, and strong intermolecular resonance interactions β to increase the electronic bandwidth W (= 4β).[4] When $W > U$, the Mott-Hubbard gap ΔE (= $U - W$) should vanish and a metallic state prevail.[5] However, while progress has been made in the development of conductive materials using highly delocalized organic radicals based on phenalenyl[6] and spirobiphenalenyl[7] frameworks, a metallic $f = {}^1/_2$ neutral radical has yet to be realized.

In pursuit of a metallic radical we have developed resonance stabilized radicals in which two 1,2,3-dithiazolyl rings are linked (Chart 1) by *N*-alkyl pyridine **1**,[8] *N*-alkyl pyrazine **2**[9] and, more recently, oxobenzene **3** bridges.[10] Increased spin delocalization reduces U, and the presence of nitrogen in spin-bearing sites helps suppress dimerization, a common fate of sterically unprotected carbon-based radicals.[11] The incorporation of sulfur, a larger and softer heteroatom, also lowers U and increases intermolecular overlap.[12] However, while variations in the R_1/R_2 ligands in **1** permit design flexibility, their steric bulk tends to buffer electronic interactions, and hence reduce bandwidth. By contrast, the less sterically encumbered radicals **2** (R = Me) and **3** (RBBO, R = Cl, Me, Ph) adopt more tightly packed structures which display increased bandwidth and improved charge transport properties.[9,10] Here we report the fluoro-substituted radical **3** (R = F), or FBBO, the layered π-stack architecture of which affords an exceptionally large bandwidth and high, albeit activated conductivity. Bandwidth enhancement by compression to 3 GPa generates a metallic state.

Chart 1

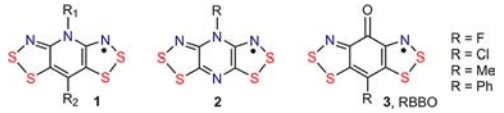

Preparation of FBBO (Figure 1) begins with the reduction of 4-fluoro-2,6-dinitrophenol **4** to the corresponding diaminophenol **5**, followed by a double Herz cyclization with sulfur monochloride. Metathesis of the crude bisdithiazolylium chloride with AgOTf provides the triflate salt [FBBO][OTf], which may be reduced with octamethylferrocene to yield purple flakes of the radical. The EPR spectrum of FBBO (in CH_2Cl_2), which consists of an overlapping doublet of pentets arising from hyperfine coupling to the two nitrogens and the basal fluorine, confirms extensive spin distribution across the molecular framework.[10] Cyclic voltammetry on [FBBO][OTf] in MeCN indicates a reversible 0/+1 couple with $E_{1/2} = 0.241$ V vs SCE. As seen in related derivatives,[10] the −1/0 couple is not reversible, but the cell potential $E_{cell} = E_{1/2}(ox) - E_{1/2}(red)$ may be estimated as the difference in the two cathodic peak potentials E_{pc}. The resulting E_{cell} value (0.69 V) is smaller than

Received: April 2, 2012
Published: June 8, 2012

   dx.doi.org/10.1021/ja303169y | *J. Am. Chem. Soc.* 2012, 134, 9886−9889

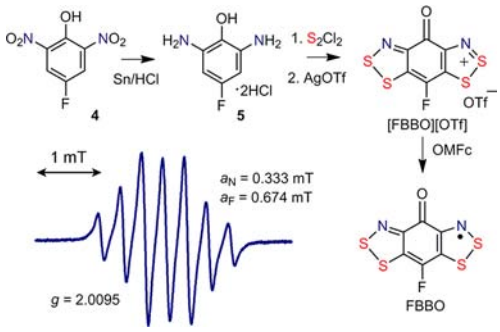

Figure 1. Synthesis and EPR spectrum (in CH_2Cl_2) of FBBO.

that typically found for **1**,[12] suggesting a lower onsite Coulomb repulsion energy $U \sim E_{cell}$.

Crystals of FBBO belong to the *C*-centered orthorhombic space group $Cmc2_1$. There are four molecules in the unit cell (Figure 2), located on crystallographic planes at $x = 0, {}^1/_2$. Within these coplanar layers, neighboring molecules along the *z*-direction are related by 2-fold screw axes. In contrast to the structures of MeBBO and the MeCN solvate of ClBBO, in which neighboring radicals are linked by lateral S···O′ and S···N′ contacts to produce ribbon-like arrays,[10] the presence of the basal fluorine in FBBO leads to a packing pattern in which the radicals are laced together in both the *y* and *z* directions by short (less than van der Waals[13]) S···O′, S···N′, and S···F′ contacts (see Supporting Information). This complex network of supramolecular synthons[14] gives rise to a rigid sheet-like architecture. Consecutive layers of radicals along the *x*-direction are related by *b*-glides at $x = {}^1/_4$ and ${}^3/_4$, which produces a "brick wall" packing pattern with an interplanar separation of *a*/2, or 3.151(1) Å.

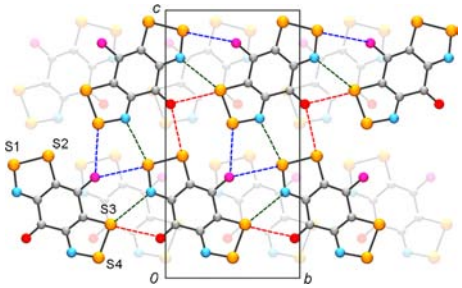

Figure 2. Unit cell of **3a** viewed parallel to the *a*-axis, showing sheet-like architecture; the layer at $x = 0.5$ is shaded. The 2D network of intermolecular S···O′ (red), S···N′ (green), and S···F′ (blue) contacts is shown with dashed lines.

The results of variable temperature magnetic susceptibility (χ) measurements on FBBO are shown in Figure 3. An initial cooling curve plot of χT vs T with $H = 1$ kOe indicated weak antiferromagnetic (AFM) exchange effects; a Curie-Weiss fit to the 50−300 K data afforded $C = 0.378$ emu K mol^{-1} and $\theta = -18.3$ K. However, on cooling below 20 K, there was a sudden increase in χT near 15 K. This surge was more pronounced at lower field ($H = 100$ Oe), and a subsequent zero-field cooled/field cooled (ZFC-FC) experiment (Figure 3b) revealed a sharp bifurcation at 13 K in χT for the ZFC and FC sweeps, which may be interpreted as a phase transition to a spin-canted AFM ordered state with a Néel temperature $T_N = 13$ K. Field independent magnetization experiments (Figure 3c) support

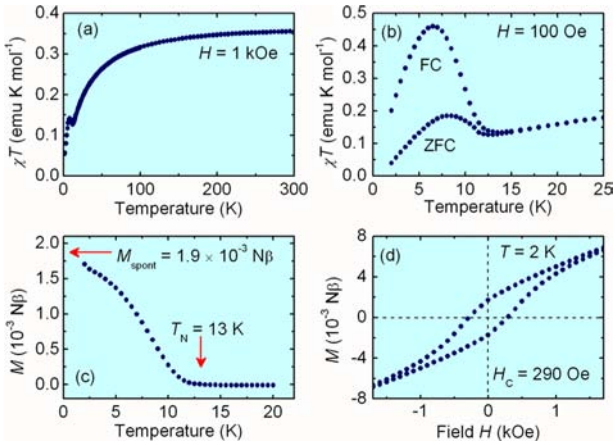

Figure 3. Magnetic measurements for FBBO. (a) Field-cooled χT vs T plot at $H = 1$ kOe. (b) ZFC-FC plot of χT vs T at $H = 100$ Oe. (c) Decay in spontaneous magnetization M with temperature, and (d) hysteresis in cycling of M vs H at $T = 2$ K.

the suggested ordering temperature, with M vanishing near 13 K, and extrapolation of M to $T = 0$ K afforded a value of the spontaneous magnetization $M_{spont} = 1.9 \times 10^{-3}$ Nβ, which was used to estimate the spin canting angle $\phi = 0.11°$. Measurements of M as a function of field indicated a weak, quasi-linear M vs H dependence out to 5 kOe. Cycling of the field revealed a hysteretic response in $M(H)$, giving rise (at 2 K) to a coercive field $H_c = 290$ Oe (Figure 3d), a surprisingly large value for a light heteroatom organic magnet.[15]

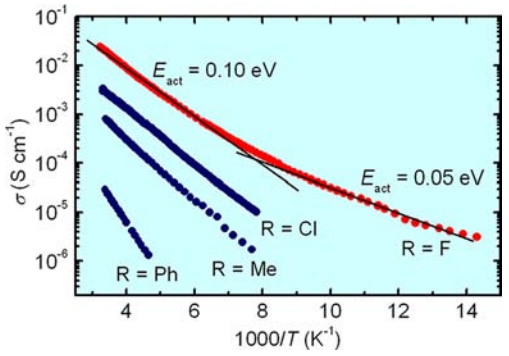

Figure 4. Plots of log σ vs $1/T$ for RBBO radicals **3**. E_{act} is shown for FBBO for $T = 150-300$ K and 70−110 K. The data for R = Cl (MeCN solvate), Me, and Ph are from ref 10.

Variable temperature, 4-probe conductivity (σ) measurements on cold-pressed pellets of FBBO have been performed at $T = 70-300$ K. The results are presented in Figure 4, along with those reported previously for other RBBO derivatives (R = Cl, Me, Ph),[10] in the form of plots of log σ vs $1/T$. While the performance of all the oxobenzene-bridged materials is uniformly superior relative to **1** in terms of both enhanced conductivity and lowered thermal activation energy E_{act}, the value of $\sigma(300\text{ K}) = 2 \times 10^{-2}$ S cm^{-1} for FBBO is, to our knowledge, the highest ever observed for a neutral $f = {}^1/_2$ radical, higher even than that of the best selenium-based variant of **1** (R_1 = Me, R_2 = Cl), for which $\sigma(300\text{ K}) = 4 \times 10^{-3}$ S cm^{-1}.[16] Moreover, while the conductivity of FBBO remains activated, indicative of a Mott-insulating ground state, the value of $E_{act} = 0.10$ eV for $T = 300-150$ K, and 0.05 eV for $T = 70-$

dx.doi.org/10.1021/ja303169y | J. Am. Chem. Soc. 2012, 134, 9886−9889

110 K constitutes the lowest ever found for a thiazyl radical. In comparison, radicals **1** show E_{act} values in the range 0.40−0.50 eV,[8] while that of the best of their selenium analogues is lowered only as far as 0.17 eV.[16]

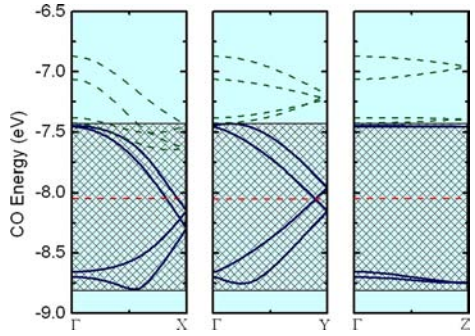

Figure 5. EHT band structure of FBBO, showing the dispersion of the four SOMO-based COs along three directions of the reciprocal unit cell. These COs would constitute the $f = {}^1/_2$ band if the ground state were metallic. The Fermi level is indicated by a dashed line (red) and the bandwidth ($W \sim 1.4$ eV) of the SOMO band is illustrated with hatching. A higher lying intruder band is also shown (dashed green).

We have explored the electronic band structure of FBBO by means of extended Hückel theory (EHT) band calculations. While this level of theory fails to provide a proper description of the ground state for strongly correlated systems, the method provides qualitative insight into the direction and extent of orbital interactions. The results (Figure 5) suggest a highly 2D electronic structure, with negligible crystal orbital (CO) dispersion along the *z*-direction (Γ→ *Z*), and strong CO dispersion along Γ→ *X* and Γ→ *Y*. The latter result may be interpreted in terms of the "brick wall" packing of the radicals in the *xy* plane, which produces a nearly isotropic square lattice of interactions (Figure 6), with four equivalent π-type intermolecular resonance integrals $\beta_1 \sim 0.22$ V. The remaining lateral interaction β_2 along the *y* direction is much smaller, near 0.02 eV. The EHT bandwidth $W \sim 1.4$ eV[17] is significantly larger than that of previously reported RBBO derivatives[10] and **1**,[8] although comparable to that for **2** (R = Me).[9] However, the electronic structure of the latter material is more 1D, and it undergoes a charge ordering distortion below 120 K to yield a diamagnetic ground state.[9] The 2D structure of FBBO appears to be resistant to such a distortion.

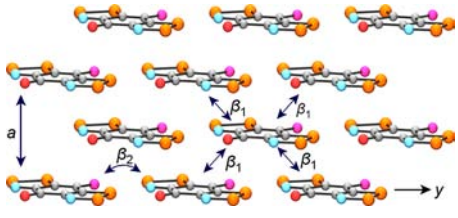

Figure 6. "Brick wall" π-stacking of FBBO radicals in the *xy* plane, illustrating the intermolecular resonance integrals β_1 and β_2.

Given the possible proximity of a metallic state, we explored the use of physical pressure to drive an insulator-to-metal phase transition. To this end, we examined the pressure dependence of the infrared absorption spectrum of FBBO, using synchrotron radiation and diamond anvil cell techniques to probe the Mott-Hubbard gap ΔE at ambient temperature. We also carried out high pressure variable temperature conductivity measurements on pressed pellets of FBBO over $T = 298$−368 K, using a cubic anvil press, to assess changes in the thermal E_{act}. At ambient pressure, the infrared spectrum of FBBO (Figure 7a) displays a series of molecular vibrational modes below 0.2 eV, but also reveals the onset of a broad hump near 0.3 eV, which we assign to ΔE. This shoulder intensifies and rapidly shifts to lower energy with increasing pressure, so that by 3 GPa the sample absorbs strongly at all photon energies within the spectral window, a finding consistent with the closure of the Mott-Hubbard gap and formation of a metallic state. The results of the high pressure conductivity measurements (Figure 7b) allow a similar conclusion. Thus, pressurization causes a steady increase in conductivity, with σ(300 K) reaching a plateau near 10^1 S cm^{-1} at about 3 GPa. Across the same pressure range, E_{act} drops sharply, vanishing near 3 GPa.

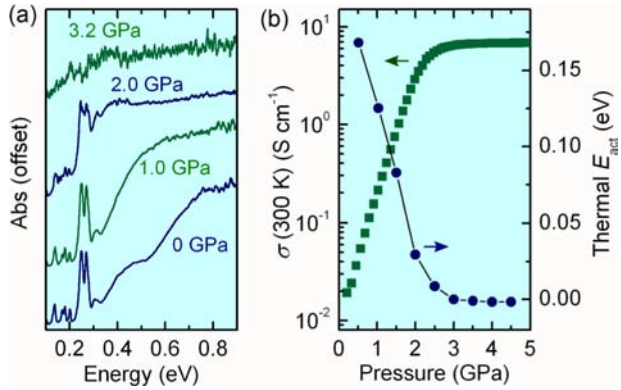

Figure 7. (a) Pressure dependence of the ambient temperature infrared absorption spectrum of FBBO; the intense band near 0.25 eV is from diamond. (b) Pressure dependence of the conductivity σ(300 K) and thermal E_{act} of FBBO.

Historically, high conductivity in radical-based materials has been achieved by doping[18] or through the design of mixed valence compounds such as spiroconjugated biphenalenyls.[7] Both strategies avoid the highly correlated $f = {}^1/_2$ state and the associated high *U* condition. The use of bandwidth enhancement alone to improve conductivity in materials that adhere to the $f = {}^1/_2$ paradigm has presented more of a challenge, largely because the approach so often leads to dimerization and a consequent loss of charge carriers. However, the unique sheet-like architecture of FBBO and the resulting interlayer π-overlap affords a high bandwidth, 2D electronic structure that resists spin-pairing. While the transport properties of FBBO indicate that the Mott insulator description still applies at ambient pressure, the insulator-to-metal transition is readily accomplished at 3 GPa, which is a considerably lower pressure than required for Se-based derivatives of **1**.[19]

In a broader context, the study of strongly correlated materials in the vicinity of the metal/insulator transition has proven useful, over the past few decades, in the search for novel properties. Thus, the transition in FBBO at room temperature is indicative of a quantum critical point in the phase diagram at a critical pressure $P_c \sim 3$ GPa and zero temperature. The physics around such points typically displays interesting features.[20] In organic charge transfer compounds, such as the

dx.doi.org/10.1021/ja303169y | J. Am. Chem. Soc. 2012, 134, 9886−9889

κ-phase salts of BEDT-TTF, the properties are tuned by a combination of physical pressure and anion substitution (chemical pressure), generating a variety of phases, including superconductivity.[21] FBBO may represent a benchmark example of a new class of strongly correlated materials based on neutral molecular radicals. Unlike charge transfer salts, where the building blocks are dimeric radical cations, neutral radicals are true $f = {}^1/_2$ materials, in which the absence of counteranions results in a simpler structure. So far, only a limited section of the phase diagram of FBBO has been examined, but already it displays properties common to these other classes of materials. That is, it possesses a highly 2D electronic structure, an ordered AFM phase at low T for $P < P_c$, and a metallic phase at high T for $P > P_c$. With further exploration of FBBO, as well as related neutral radical materials, there is little doubt that interesting physics will emerge.

■ ASSOCIATED CONTENT

Ⓢ Supporting Information

Experimental details and characterization data. This material is available free of charge via the Internet at http://pubs.acs.org.

■ AUTHOR INFORMATION

Corresponding Author

oakley@uwaterloo.ca

Notes

The authors declare no competing financial interest.

■ ACKNOWLEDGMENTS

We thank the NSERC (Canada) and the EPSRC (U.K., Grant No: EP/C536436/1) for financial support, a NSERC postdoctoral fellowship to C.M.R. and a NSERC graduate scholarship to S.M.W. We also thank the Government of Canada for a Tier I Canada Research Chair to J.S.T., the Diamond Light Source for beam time and Professor Bill Clegg for help with processing the DLS data.

■ REFERENCES

(1) (a) Haddon, R. C. *Nature* **1975**, *256*, 394. (b) Haddon, R. C. *Aust. J. Chem.* **1975**, *28*, 2333. (c) Haddon, R. C. *Aust. J. Chem.* **1975**, *28*, 2343.

(2) The importance of avoiding $f = {}^1/_2$ states was well established early on in the development of charge transfer conductors. See (a) Torrance, J. B. *Acc. Chem. Res.* **1979**, *12*, 79. (b) Garito, A. F.; Heeger, A. J. *Acc. Chem. Res.* **1974**, *7*, 232.

(3) (a) Eley, D. D.; Jones, K. W.; Littler, J. G. F.; Willis, M. R. *Trans. Faraday Soc.* **1966**, *62*, 3192. (b) Inokuchi, H.; Harada, Y.; Maruyama, Y. *Bull. Chem. Soc. Jpn.* **1962**, *35*, 1559.

(4) (a) Tian, Y.; Kertesz, M. *J. Am. Chem. Soc.* **2010**, *132*, 10648. (b) Vérot, M.; Rota, J.-B.; Kepenekian, M.; Le Guennica, B.; Robert, V. *Phys. Chem. Chem. Phys.* **2011**, *13*, 6657.

(5) (a) Mott, N. F. *Proc. Phys. Soc. A* **1949**, *62*, 416. (b) Mott, N. F. *Metal-Insulator Transitions*; Taylor and Francis: London, 1990. (c) Hubbard, J. *Proc. R. Soc. London* **1963**, *A276*, 238.

(6) (a) Haddon, R. C.; Wudl, F.; Kaplan, M. L.; Marshall, J. H.; Cais, R. E.; Bramwell, F. B. *J. Am. Chem. Soc.* **1978**, *100*, 7629. (b) Goto, K.; Kubo, T.; Yamamoto, K.; Nakasuji, K.; Sato, K.; Shiomi, D.; Takui, T.; Kubota, M.; Kobayashi, T.; Yakusi, K.; Ouyang, J. *J. Am. Chem. Soc.* **1999**, *121*, 1619. (c) Koutentis, P. A.; Chen, Y.; Cao, Y.; Best, T. P.; Itkis, M. E.; Beer, L.; Oakley, R. T.; Cordes, A. W.; Brock, C. P.; Haddon, R. C. *J. Am. Chem. Soc.* **2001**, *123*, 3864. (d) Morita, Y.; Suzuki, S.; Sato, K.; Takui, T. *Nat. Chem.* **2011**, *3*, 197. (e) Kubo, T.; Katada, Y.; Shimizu, A.; Hirao, Y.; Sato, K.; Takui, T.; Uruichi, M.; Yakushi, K.; Haddon, R. C. *J. Am. Chem. Soc.* **2011**, *133*, 14240.

(7) High room temperature conductivity ($\sigma \sim 0.3$ S cm^{-1}) has been observed in some spirobiphenalenyls, but these mixed valence systems may be viewed as $f = {}^1/_4$ materials. See (a) Chi, X.; Itkis, M. E.; Patrick, B. O.; Barclay, T. M.; Reed, R. W.; Oakley, R. T.; Cordes, A. W.; Haddon, R. C. *J. Am. Chem. Soc.* **1999**, *121*, 10395. (b) Mandal, S. K.; Samanta, S.; Itkis, M. E.; Jensen, D. W.; Reed, R. W.; Oakley, R. T.; Tham, F. S.; Donnadieu, B.; Haddon, R. C. *J. Am. Chem. Soc.* **2006**, *128*, 1982. (c) Pal, S. K.; Itkis, M. E.; Tham, F. S.; Reed, R. W.; Oakley, R. T.; Haddon, R. C. *Science* **2005**, *309*, 281. (d) Bag, P.; Itkis, M. E.; Pal, S. K.; Donnadieu, B.; Tham, F. S.; Park, H.; Schlueter, J. A.; Siegrist, T.; Haddon, R. C. *J. Am. Chem. Soc.* **2010**, *132*, 2684.

(8) (a) Beer, L.; Brusso, J. L.; Cordes, A. W.; Haddon, R. C.; Itkis, M. E.; Kirschbaum, K.; MacGregor, D. S.; Oakley, R. T.; Pinkerton, A. A.; Reed, R. W. *J. Am. Chem. Soc.* **2002**, *124*, 9498. (b) Beer, L.; Britten, J. F.; Brusso, J. L.; Cordes, A. W.; Haddon, R. C.; Itkis, M. E.; MacGregor, D. S.; Oakley, R. T.; Reed, R. W.; Robertson, C. M. *J. Am. Chem. Soc.* **2003**, *125*, 14394. (c) Beer, L.; Britten, J. F.; Clements, O. P.; Haddon, R. C.; Itkis, M. E.; Matkovich, K. M.; Oakley, R. T.; Reed, R. W. *Chem. Mater.* **2004**, *16*, 1564.

(9) Leitch, A. A.; Reed, R. W.; Robertson, C. M.; Britten, J. F.; Yu, X.; Secco, R. A.; Oakley, R. T. *J. Am. Chem. Soc.* **2007**, *129*, 7903.

(10) (a) Yu, X.; Mailman, A.; Dube, P. A.; Assoud, A.; Oakley, R. T. *Chem. Commun.* **2011**, *47*, 4655. (b) Yu, X.; Mailman, A.; Lekin, K.; Assoud, A.; Robertson, C. M.; Noll, B. C.; Campana, C. F.; Howard, J. A. K.; Dube, P. A.; Oakley, R. T. *J. Am. Chem. Soc.* **2012**, *134*, 2264. (c) Yu, X.; Mailman, A.; Lekin, K.; Assoud, A.; Dube, P. A.; Oakley, R. T. *Cryst. Growth Des.* **2012**, *12*, 2485.

(11) (a) Takui, T.; Kubota, M.; Kobayashi, T.; Yakusi, K.; Ouyang, J. *J. Am. Chem. Soc.* **1999**, *121*, 1619. (b) Small, D.; Zaitsev, V.; Jung, Y.; Rosokha, S. V.; Head-Gordon, M.; Kochi, J. K. *J. Am. Chem. Soc.* **2004**, *126*, 13850. (c) Beer, L.; Mandal, S. K.; Reed, R. W.; Oakley, R. T.; Tham, F. S.; Donnadieu, B.; Haddon, R. C. *Cryst. Growth Des.* **2007**, *7*, 802.

(12) Cordes, A. W.; Haddon, R. C.; Oakley, R. T. *Phosphorus, Sulfur, Silicon Relat. Elem.* **2004**, *179*, 673.

(13) Bondi, A. *J. Phys. Chem.* **1964**, *68*, 441.

(14) Desiraju, G. R. *Angew. Chem., Int. Ed. Engl.* **1995**, *34*, 23113.

(15) (a) Rawson, J. M.; Alberola, A.; Whalley, A. *J. Mater. Chem.* **2006**, *16*, 2560. (b) Lahti, P. *Adv. Phys. Org. Chem.* **2011**, *45*, 93. (c) Ratera, I.; Veciana, J. *Chem. Soc. Rev.* **2012**, *41*, 303.

(16) Leitch, A. A.; Yu, X.; Winter, S. M.; Secco, R. A.; Dube, P. A.; Oakley, R. T. *J. Am. Chem. Soc.* **2009**, *131*, 7112.

(17) The EHT method probably overestimates the bandwidth of FBBO. Preliminary DFT calculations suggest a smaller W, in keeping with the measured valence band photoelectron spectrum and the value of U estimated electrochemically. Tse, J. S., unpublished results.

(18) (a) Bryan, C. D.; Cordes, A. W.; Haddon, R. C.; Glarum, S. H.; Hicks, R. G.; Kennepohl, D. K.; MacKinnon, C. D.; Oakley, R. T.; Palstra, T. T. M.; Perel, A. S.; Schneemeyer, L. F.; Scott, S. R.; Waszczak, J. V. *J. Am. Chem. Soc.* **1994**, *116*, 1205. (b) Bryan, C. D.; Cordes, A. W.; Fleming, R. M.; George, N. A.; Glarum, S. H.; Haddon, R. C.; MacKinnon, C. D.; Oakley, R. T.; Palstra, T. T. M.; Perel, A. S. *J. Am. Chem. Soc.* **1995**, *117*, 6880.

(19) Leitch, A. A.; Lekin, K.; Winter, S. M.; Downie, L. E.; Tsuruda, H.; Tse, J. S.; Mito, M.; Desgreniers, S.; Dube, P. A.; Zhang, S.; Liu, Q.; Jin, C.; Ohishi, Y.; Oakley, R. T. *J. Am. Chem. Soc.* **2011**, *133*, 6051.

(20) (a) Norman, M. R. *Science* **2011**, *332*, 196. (b) Si, Q.; Steglich, F. *Science* **2010**, *329*, 1161. (c) Coleman, P.; Schofield, A. J. *Nature* **2005**, *433*, 226. (d) Dressel, M. *J. Phys.: Condens. Matter* **2011**, *23*, 293201.

(21) (a) Ito, H.; Ishiguro, T.; Kubota, M.; Saito, G. *J. Phys. Soc. Jpn.* **1996**, *65*, 2987. (b) McKenzie, R. H. *Science* **1997**, *278*, 820. (c) Day, P.; Kurmoo, M.; Mallah, T.; Marsden, I. R.; Friend, R. H.; Pratt, F. L.; Hayes, W.; Chasseau, D.; Gaultier, J.; Bravic, G.; Ducasse, L. *J. Am. Chem. Soc.* **1992**, *114*, 10722. (d) Limelette, P.; Wzietek, P.; Florens, S.; Georges, A.; Costi, T. A.; Pasquier, C.; Jérome, D.; Mézière, C.; Batail, P. *Phys. Rev. Lett.* **2003**, *91*, 016401. (e) Saito, G.; Yoshida, Y. *Bull. Chem. Soc. Jpn.* **2007**, *80*, 1. (f) Nam, M.-S; Ardavan, A.; Blundell, S. J.; Schlueter, J. A. *Nature* **2007**, *449*, 584.